Propagation of partially coherent light in non-Hermitian lattices

P. A. Brandão * and J. C. A. Rocha
Instituto de Física, Universidade Federal de Alagoas, Maceió 57072-900, Brazil

(Received 25 July 2022; accepted 18 November 2022; published 6 December 2022)

Band theory for partially coherent light is introduced by using the formalism of second-order classical coherence theory. It is demonstrated that the cross-spectral density function can have bands and gaps and form a correlation band structure. The propagation of a partially coherent beam in non-Hermitian periodic structures is considered to elucidate the interplay between the degree of coherence and the gain or loss present in the lattice. We apply the formalism to study partially coherent Bloch oscillations in lattices having parity-time symmetry.

DOI: 10.1103/PhysRevA.106.063503

I. INTRODUCTION

It has been recognized for a long time that the coherence of optical wave fields is one of the main features that dictates how the field will evolve and interact with matter [1]. The importance of considering the optical coherence properties is reflected in the numerous developments in technological applications, such as optical coherence tomography [2], which enabled noninvasive cross-section imaging of biological tissues, trapping of dielectric particles [3], with the advantage of using beams with low intensity such that biological samples are not damaged, photovoltaics [4], where the coherence properties of sunlight are investigated along with its harvesting at the Earth's surface, to cite a few [5].

Since the interaction between radiation and matter is ubiquitous in nature, each development of a novel class of dielectric materials is followed by the investigation of the dynamics of light propagation through such media. In this view, there has been enormous interest in so-called non-Hermitian materials, which represent another class of dielectrics that can give to or take energy from the optical wave in a controlled manner [6,7]. Apparently, the most successful subclass of non-Hermitian materials that has been proven to give new and unique optical effects is the subclass having the property of parity-time ($\mathcal{PT}$) symmetry [8,9].

Despite the large amount of investigations regarding propagation of optical beams in complex materials, the role of the degree of coherence and its relation to $\mathcal{PT}$-symmetric structures has not yet been fully explored. In fact, the interaction between partially coherent classical light and materials having $\mathcal{PT}$ symmetry has just started to be considered in scattering systems [10–19]. These initial results provide strong evidence to the fact that the interplay between gain, loss, and the degree of coherence is not trivial and that coherence-induced non-Hermitian effects can be controlled in such systems. We hope that the results reported here may place classical coherence theory into a more robust framework in the context of non-Hermitian photonics.

*paulo.brandao@fis.ufal.br

II. PROPAGATION OF PARTIALLY COHERENT BEAMS

Let us begin by considering the stochastic optical field $u(x, z, t)$ in the scalar approximation and assume that it only depends on the x and z spatial coordinates with the z axis denoting the main propagation direction. A monochromatic component of $u(x, z, t)$ with frequency ω is written as $\psi(x, z, \omega)$ with the dependence on ω being suppressed from now on. Suppose the beam propagates in a paraxial condition such that $\psi(x, z)$ satisfies the paraxial wave equation (written in scaled units [20]),

$$i\frac{\partial\psi(x,z)}{\partial z} = \frac{1}{2}\frac{\partial^2\psi(x,z)}{\partial x^2} + V(x)\psi(x,z), \tag{1}$$

where $V(x)$ is the complex potential function related to the refractive index of the structure [8]. In second-order classical coherence, we characterize the beam dynamics through the cross-spectral density function $W(x_1, x_2, z)$ defined as [1]

$$W(x_1, x_2, z) = \langle\psi^*(x_1, z)\psi(x_2, z)\rangle_\omega, \tag{2}$$

where the average is taken over an ensemble of functions of monochromatic components. Being a field function, the cross-spectral density must evolve according to a differential equation, which is obtained by taking the derivative of (2) with respect to z and using (1),

$$i\frac{\partial W}{\partial z} + \frac{1}{2}\left(\frac{\partial^2 W}{\partial x_1^2} - \frac{\partial^2 W}{\partial x_2^2}\right) + \mathcal{V}(x_1, x_2)W = 0, \tag{3}$$

where $\mathcal{V}(x_1, x_2) = V^*(x_1) - V(x_2)$ is an effective potential function for the cross-spectral density. A more general differential equation has been derived to describe the evolution of partially coherent light in nonlinear media [21,22]. The partial differential equation (3) indicates that if the optical field $\psi(x, z)$ evolves under the potential $V(x)$, its cross-spectral density $W(x_1, x_2, z)$ must evolve under the effective potential $\mathcal{V}(x_1, x_2)$. Apart from the difference between the sign in the second-order derivative in x, (3) is essentially a (2+1)-dimensional description of paraxial wave beams $U(x, y, z)$ propagating in the z direction through a material described by the transverse refractive index profile $\mathcal{V}(x, y)$.

Contrary to the case of monochromatic and fully coherent beams, the cross-spectral density cannot be chosen arbitrarily. It must satisfy the non-negative definiteness condition $\int W(\mathbf{r}_1,\mathbf{r}_2)f^*(\mathbf{r}_1)f(\mathbf{r}_2)d\mathbf{r}_1 d\mathbf{r}_2 \geqslant 0$ for any choice of well-behaved functions $f(\mathbf{r})$ [1]. A sufficient condition for constructing such genuine correlation functions is obtained by writing [23]

$$W(x_1,x_2,z)=\int p(v)H^*(x_1,z,v)H(x_2,z,v)dv, \quad (4)$$

where $p(v)>0$ and $H(x,z,v)$ is an arbitrary Kernel. Notice that the spectral density $S(x)=W(x,x,z)=\langle|\psi(x,z)|^2\rangle_\omega$ is always positive, independent of the particular form of $H(x,z,v)$. Representation (4) also guarantees that the degree of coherence $\mu(x_1,x_2,z)$, defined by

$$\mu(x_1,x_2,z)=\frac{W(x_1,x_2,z)}{[S(x_1,x_1,z)S(x_2,x_2,z)]^{1/2}}, \quad (5)$$

satisfies $0\leqslant|\mu(x_1,x_2,z)|\leqslant 1$ such that it can be used to characterize the spatial coherence of the field between positions (x_1,z) and (x_2,z). In dealing with the propagation of paraxial beams, we choose $H(x,z,v)=\int\tilde{w}(k,z,v)e^{ikx}dk$ such that the representation for $W(x_1,x_2,z)$ acquires the interesting form

$$W(x_1,x_2,z)=\iint dk_1dk_2w(k_1,k_2,z)e^{i(k_2x_2-k_1x_1)}, \quad (6)$$

where $w(k_1,k_2,z)=\int\tilde{w}^*(k_1,z,v)\tilde{w}(k_2,z,v)p(v)dv$.

III. BAND THEORY FOR PARTIALLY COHERENT LIGHT

Considering a periodic material described by the complex-valued potential function $V(x)=\alpha\sum_{n=-\infty}^{\infty}c_ne^{2\pi inx/L}$, where c_n and α are real-valued parameters, L is the lattice period and after substituting (6) into (3), we obtain the differential equation governing the evolution of $w(k_1,k_2,z)$:

$$i\frac{dw(k_1,k_2,z)}{dz}=\frac{1}{2}\left(k_1^2-k_2^2\right)w(k_1,k_2,z)+\alpha\sum_{n=-\infty}^{\infty}c_n\left[w\left(k_1,k_2-\frac{2\pi n}{L},z\right)-w\left(k_1-\frac{2\pi n}{L},k_2,z\right)\right]. \quad (7)$$

Notice how the definition of $w(k_1,k_2,z)$ implies the symmetry $w(k_1,k_2,z)=w^*(k_2,k_1,z)$ which is already satisfied by (7). This equation indicates that the lattice couples the k-space cross-spectral density of the incident beam into discrete regions in the (k_1,k_2) plane during propagation. We call attention to the fact that this is very similar to the standard theory of coherent waves propagating in two-dimensional periodic lattices, but here this coupling happens in the correlation function while the physical system is intrinsic (1+1)-dimensional. Furthermore, the negative sign present in the Laplacian operator (which is reflected in the $k_1^2-k_2^2$ term) introduces several changes in the band structure of the system and in the propagation properties of the field, as described next.

In the absence of the lattice, the general solution of (7) is given by $w_{\alpha=0}(k_1,k_2,z)=w_{\alpha=0}(k_1,k_2,0)e^{-(i/2)(k_1^2-k_2^2)z}$,

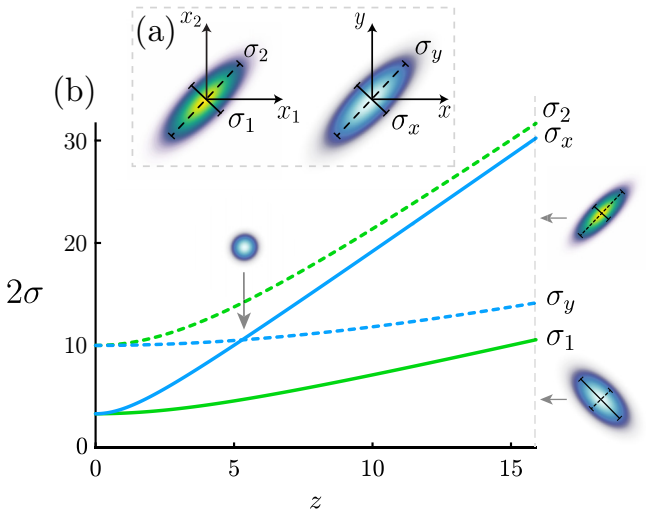

FIG. 1. Comparison between the beam waist $\sigma_{1,2}$ of $W(x_1,x_2,z)$ and $\sigma_{x,y}$ of $U(x,y,z)$ in the diagonal positions $x_1\pm x_2=0$ and $x\pm y=0$ during propagation in free space. (a) Initial profiles at $z=0$ given by the same function $f(\xi_1,\xi_2,0)=e^{-(\xi_1^2+\xi_2^2)/2\delta^2}e^{-(\xi_1-\xi_2)^2/2\Delta^2}$ with $W(x_1,x_2,z)$ evolving according to (3) and $U(x,y,z)$ propagating with the same equation but with a plus sign in the Laplacian term (standard paraxial propagation). (b) The position where the blue curves cross indicates that $\sigma_x=\sigma_y$ so that the beam $U(x,y,z)$ becomes symmetrical. This crossing never occurs for $W(x_1,x_2,z)$. Parameters used: $\delta=10$ and $\Delta=5$.

where the exponential factor closely resembles the Fourier propagator for (2+1) coherent systems. A similar propagator appears in a distinct system as the Fourier propagator for a TM polarized harmonic mode in homogeneous but anisotropic media [24]. Figure 1 shows the main difference between the free-space propagation of a monochromatic beam $U(x,y,z)$, evolving under the standard paraxial wave equation, and the cross-spectral density $W(x_1,x_2,z)$, evolving under (3) with $\mathcal{V}=0$, when both are given the same initial asymmetrical field distribution. The figure plots the evolution of the beam widths ($\sigma_{1,2}$ for W and $\sigma_{x,y}$ for U) along the two main diagonals of the field ($x_1\pm x_2=0$ and $x\pm y=0$), defined as twice the second moment of the intensity distribution [25].

Consider now the effects of the lattice. Without loss of generality, assume that the potential $V(x)$ has only three nonzero Fourier components, c_0, $c_{\pm1}$, and write $c_0=1$ and $c_{\pm1}=\frac{1}{2}(1\pm\gamma)$ where $\gamma\geqslant 0$. The Hermitian configuration with real V is recovered if $\gamma=0$ and for $\gamma\neq 0$ the potential is $\mathcal{PT}$-symmetric with $\gamma=1$ being the symmetry breaking point. Let us now try to define a coherence band structure, analogous to the usual band structure of coherent waves, by writing $w(k_1,k_2,z)=p(k_1,k_2)e^{i\beta z}$, where β is the coherence eigenvalue, and substituting this form into (7). The coherence band structure for $\alpha=0$ is seen to be $\beta=\frac{1}{2}(k_2^2-k_1^2)$, described by a hyperbolic paraboloid, which has a very different topology when compared to the band structure of a two-dimensional coherent beam (described by a paraboloid) due to the minus sign in the expression.

This unusual topology has its origin in the fact that, from the symmetry requirement $w(k_1,k_2,z)=w^*(k_2,k_1,z)$, the necessary condition $\beta=0$ must be satisfied whenever

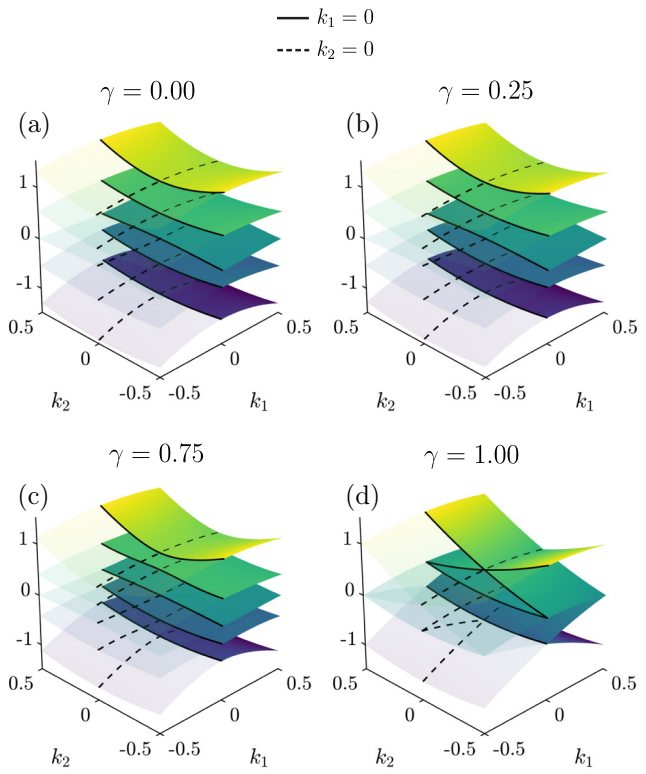

FIG. 2. Coherence band structures for partially coherent light in non-Hermitian lattices with (a) $\gamma = 0$ (Hermitian lattice), (b) $\gamma = 0.25$ and (c) $\gamma = 0.75$ ($\mathcal{PT}$-symmetric lattices below threshold), and (d) $\gamma = 1$ ($\mathcal{PT}$-symmetric lattice at the symmetry breaking point). The bands in the last case are identical with the bands in the absence of the lattice $\alpha = 0$. The lattice period is $L = 2\pi$.

$k_1 = k_2$. This is because $w(k, k, z)$ has to be a real-valued function. No such requirements are needed when considering the usual coherent propagation because $U(x, y, z)$ does not represent a correlation function. Therefore, the necessity of the cross-spectral density to be a genuine correlation profile changes the topology of the coherence band structure. Figure 2 shows the plots of the band structure for several values of γ. Part (d) of this figure indicates the symmetry breaking point where the band merging occurs. Clearly, non-Hermiticity can influence the propagation of partially coherent beams in a nontrivial way. The connection between band gaps and classical coherence has recently been emphasized in the context of plasmonics [26].

In this view, one can still form correlation wave packets by linear combinations of $p_n(k_1, k_2)e^{i\beta_n z}$ as long as $w(k_1, k_2, z) = w^*(k_2, k_1, z)$. It is thus necessary that for every positive eigenvalue $\beta_n(k, k)$ present in the wave packet there is a corresponding negative one $-\beta_n(k, k)$. The band diagram must reflect this symmetry and Fig. 3 highlights the eigenvalues along the diagonal $k_1 = k_2$ to confirm these claims. This explains why the bands are symmetrical with respect to $\beta = 0$ along the $k_1 = k_2$ axis.

The significance of the coherence eigenstates $w_n(k_1, k_2, z)$ becomes clear if we consider the k-space degree of coherence $\mu_w^{(n)}(k_1, k_2, z) = w_n(k_1, k_2, z)/[w_n(k_1, k_1, z)w_n(k_2, k_2, z)]^{1/2}$, defined in analogy with the spectral degree of coherence,

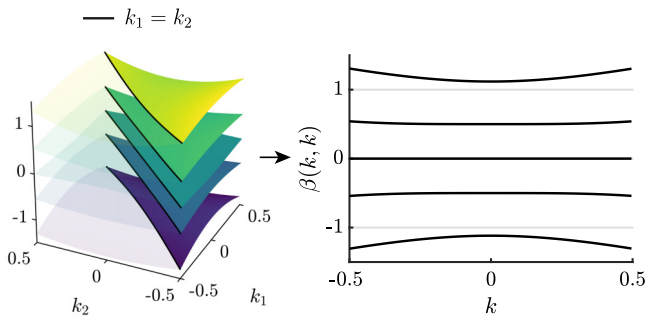

FIG. 3. Cross section along the diagonal ($k_1 = k_2$) of the band diagram for $\gamma = 0.5$. This figure indicates the symmetrical distribution of the positive and negative coherence eigenvalues β.

and note that $|\mu_w^{(n)}|$ is independent of z, which is the partially coherent version of the stationary states present in the usual band theory for coherent states.

IV. BEAM DYNAMICS

It is now time to discuss some beam dynamics. Consider a beam having finite transverse extent δ propagating in the complex lattice $V(x)$. The beam is assumed to be initiated at $z = 0$ and described by the Gaussian-Schell model with the cross-spectral density $W(x_1, x_2, 0)$ given by

$$W(x_1, x_2, 0) = S_0 e^{-(x_1^2+x_2)^2/2\delta^2} e^{-(x_1-x_2)^2/2\Delta^2}, \tag{8}$$

where δ is related to the beam width at $z = 0$ and Δ is the spatial coherence parameter which controls the statistical correlations between positions x_1 and x_2. The spectral density is given by a Gaussian function $S(x, 0) = W(x, x, 0) = S_0 e^{-x^2/\delta^2}$, where S_0 is the amplitude of the incident beam. From (5) we obtain the spatial degree of coherence, $\mu(x_1 - x_2) = e^{-(x_1-x_2)^2/2\Delta^2}$. The beam is said to be fully coherent in the limit $\Delta \to \infty$ ($\mu \to 1$) where $W(x_1, x_2)$ becomes a separable function, as can be verified. We are mainly interested in the relationship between the coherence parameter Δ and the non-Hermitian lattice and how they influence the beam propagation through the material.

For the Gaussian-Schell model (8), the function $w(k_1, k_2, 0)$ can be calculated directly from (6). It is given by

$$w(k_1, k_2, 0) = \frac{2\pi S_0 \delta^2 \Delta}{\sqrt{2\delta^2 + \Delta^2}} \exp\left\{ -\frac{\delta^2}{2(2\delta^2 + \Delta^2)} \times \left[(k_1 - k_2)^2\delta^2 + (k_1^2 + k_2^2)\Delta^2\right]\right\}, \tag{9}$$

which can be used as the initial condition in (7). However, it is more efficient to solve (3) directly by using split-step Fourier numerical methods, with an absorbing material on the boundaries to prevent reflection of the outgoing modes, and use (8) as the initial condition [27]. We also compared all numerical results with second-order perturbation theory and obtained an excellent agreement. Figure 4 shows the evolution of the spectral density $S(x, z)$ (right panels), along with $w(k_1, k_2, z)$ (left panels), for a passive $\gamma = 0$ and $\mathcal{PT}$-symmetric $\gamma = 1$ lattice. In the Hermitian case with (large) spatial coherence

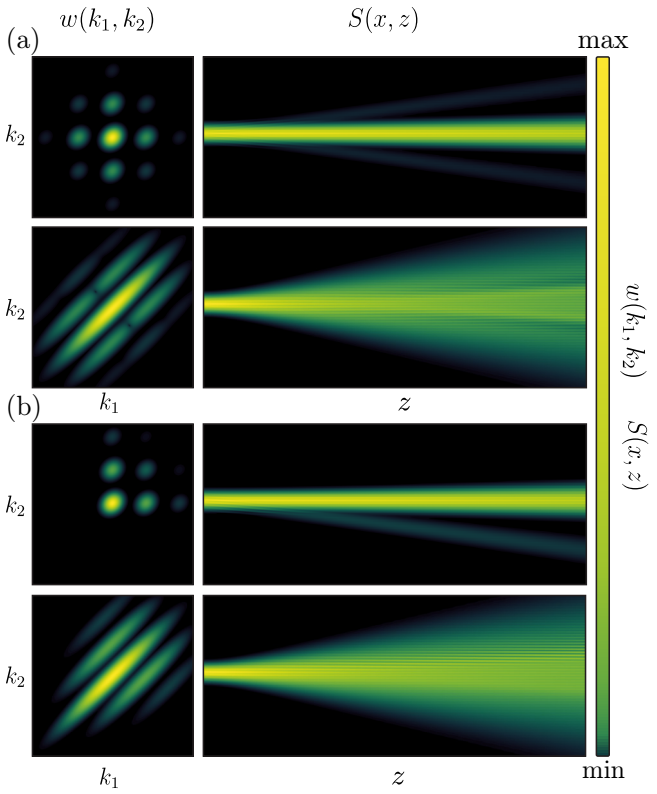

FIG. 4. Double refraction of a Gaussian-Schell beam propagating in Hermitian and non-Hermitian lattices. (a) Hermitian lattice with $\gamma = 0$ and (top) $\Delta = 20$, (bottom) $\Delta = 2$. The spectral correlation function $w(k_1, k_2, z)$ couples to the lattice according to (7). (b) Evolution in a non-Hermitian lattice with $\gamma = 1$. In both cases the k-space correlation function broadens as the degree of spatial coherence decreases, washing out any non-Hermitian effects on its propagation. The incident beam width remained fixed at $\delta = 10$. The left panels display $|w(k_1, k_2, z)|^2$ evaluated at $z = 0.5$. The initial distribution at $z = 0$ is given by Eq. (9) in both cases. All plotted quantities are dimensionless.

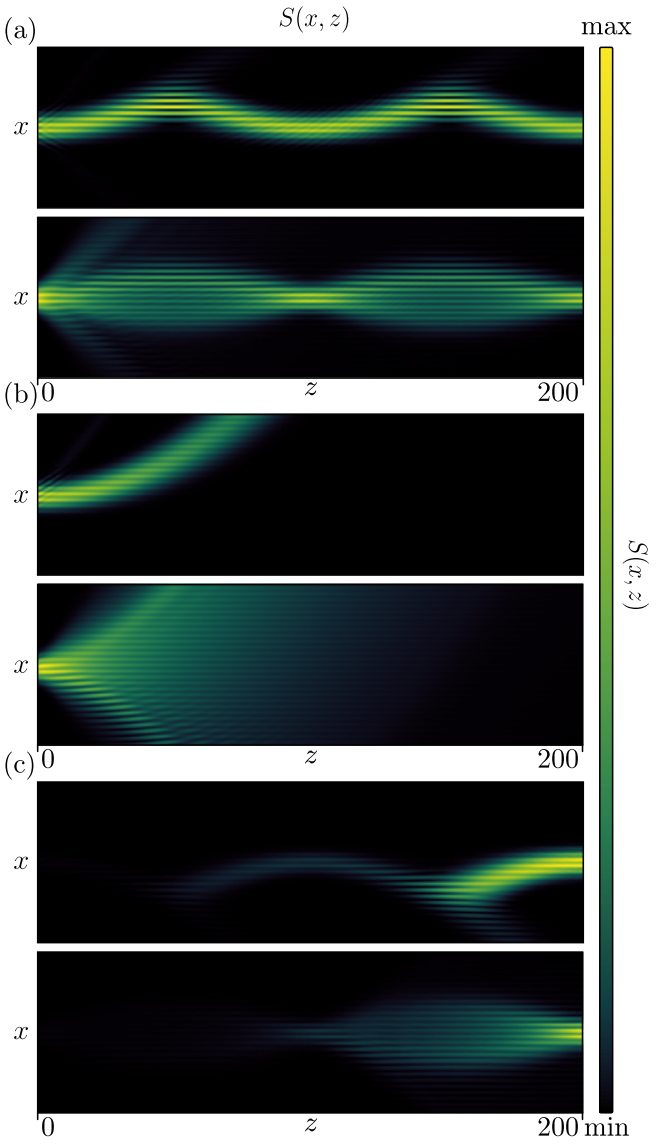

FIG. 5. Bloch oscillations with partially coherent light in complex media. (a) Coherence-induced transition between oscillating and breathing modes with $\gamma = 0$, (top) $\Delta = 100$, and (bottom) $\Delta = 2$. (b) Evolution through the lattice at the symmetry breaking point $\gamma = 1$ with (top) $\Delta = 100$ and (bottom) $\Delta = 2$. In both cases the initial beam width is $\delta = 10$, $L = 2\pi$, and $\alpha = 5 \times 10^{-3}$. In panels (a) and (b) $\beta = -0.2 \times 10^{-3}$, and for panel (c) $\beta = 0.2 \times 10^{-3}$ with $\gamma = 1$. All plotted quantities are dimensionless.

$\Delta = 20$, we see in the top panel of Fig. 4(a) the usual Bragg diffraction with symmetrical first-order modes, which reflects the symmetry of the coherence lattice $w(k_1, k_2, z)$. However, as the degree of spatial coherence decreases, the once discrete Bragg modes merge in a symmetric way along the diagonal $k_1 = k_2$ and the overall effect of the Bragg modes is washed out during propagation.

In the case of a lattice having gain and loss at the symmetry breaking point $\gamma = 1$, and large coherence, a few of the Bragg modes are not excited and the beam evolution displays the phenomenon of double refraction [20], as can be seen in Fig. 4(b). However, as Δ decreases, the spatial correlation induces the creation of new modes in such a way that the observed double refraction is destroyed, albeit in a more asymmetrical way. The curious pattern of diagonal stripes can be understood by noticing that in the $\Delta \to 0$ limit, the cross-spectral density function must behave as $W(x_1, x_2, z) \propto \delta(x_1 - x_2)$ and from (3) we concluded that $w(k_1, k_2, z)$ depends only on the difference between k_1 and k_2. We emphasize that the initial beam width is the same in all simulations, so it is indeed the spatial correlation that is exciting new modes.

As the previous results suggest, the broadening in the correlation space as Δ decreases, i.e., as the beam becomes more spatially incoherent, can lead to a nontrivial dynamics and excitation of a large number of modes for a fixed initial beam width. In order to show a more dramatic example, consider adding a linear ramp to the periodic lattice, thus breaking the periodic symmetry of the material. More quantitatively, let us consider the propagation of the Gaussian-Schell beam (8) through the potential $V(x) = \alpha \sum_{n=-\infty}^{\infty} c_n e^{2\pi i n x/L} + \beta x$,

where β is a constant parameter, again with $c_0 = 1$, $c_{\pm 1} = \frac{1}{2}(1 \pm \gamma)$, and $c_n = 0$ ($|n| > 1$).

Figure 5 plots the beam evolution by numerically solving (3). Part (a) displays the Hermitian case with (top panel) large $\Delta = 100$ and (bottom panel) small $\Delta = 2$ spatial coherence for a fixed beam width $\delta = 10$. We observe a coherence-induced transition between oscillating and breathing modes of Bloch oscillations as $\Delta \to 0$. To explain this, recall that the breathing mode is observed in fully coherent systems as the incident beam width decreases [28,29]. The initial beam width of our simulation remained fixed at $\delta = 10$. However, in the correlation space (k_1, k_2), the overall area of the beam width (which is composed of δ and Δ) actually decreases as $\Delta \to 0$. In other words, less modes are initially excited in the $\Delta \to 0$ limit. Since it is the spatial correlation that determines the beam evolution, the role of the partial coherence is reflected in the real-space propagation of the spectral density $S(x, z) = W(x, x, z)$.

In the case of a lattice at the symmetry breaking point $\gamma = 1$, (3) is able to describe the usual behavior of an accelerating beam, shown in the top panel of Fig. 5(b), as if propagating in free space. In the low coherence regime, shown in the bottom panel, the partially coherent beam spreads strongly, albeit in a more skewed distribution. This suggests that it is possible to control, and even cancel, the accelerating effect present in fully coherent systems. These results were obtained by considering β negative. The case with $\beta > 0$ is shown in Fig. 5(c) where the top panel shows the beam evolution in the case of high coherence. In this case, the beam amplitude increases during propagation, which is a well-known result [29]. The bottom panel displays the analogous breathing mode, where the amplitude also increases during propagation, as the spatial coherence decreases. These results are direct generalizations of previous studies [29] when the beam is no longer fully (spatially) coherent.

V. CONCLUSIONS

The inclusion of partial coherence in optical systems can generate new dynamics not present in the fully coherent counterparts. In the same way that a real Hermitian theory can be extended to the complex non-Hermitian domain, a fully coherent theory can be made partially coherent by introducing the cross-spectral density function, as done here. In this respect, every theory reported involving propagation of beams through inhomogeneous media in paraxial conditions, can be generalized to include the role of the degree of coherence. The formalism can be easily generalized to include a z-dependent potential function, which has important applications in photonics [30,31]. Our results provide a step towards an understanding between the role of spatial coherence and complex media in paraxial conditions.

ACKNOWLEDGMENTS

The authors acknowledge the financial support of Conselho Nacional de Desenvolvimento Científico e Tecnológico (CNPq). We also thank S. B. Cavalcanti for a critical reading of the preprint and one of the referees for calling our attention to the similarity between the free-space propagator for the cross-spectral density function and the Fourier propagator for hyperbolic media [24].

[1] L. Mandel and E. Wolf, *Optical Coherence and Quantum Optics* (Cambridge University Press, Cambridge, UK, 1995).

[2] D. Huang, E. Swanson, C. Lin, J. Schuman, W. Stinson, W. Chang, M. Hee, T. Flotte, K. Gregory, C. Puliafito *et al.*, Optical coherence tomography, Science **254**, 1178 (1991).

[3] J. M. Aunon and M. Nieto-Vesperinas, Optical forces on small particles from partially coherent light, J. Opt. Soc. Am. A **29**, 1389 (2012).

[4] M. K. Chaudhari, B. K. Singh, and P. C. Pandey, Enhanced light trapping in dye-sensitized solar cell by coupling to 1D photonic crystal and accounting for finite coherence length, J. Mod. Opt. **64**, 2385 (2017).

[5] O. Korotkova and G. Gbur, Applications of optical coherence theory, in *Progress in Optics: A Tribute to Emil Wolf*, edited by T. D. Visser (Elsevier, New York, 2020), Vol. 65, Chap. 4, pp. 43–104.

[6] C. E. Rüter, K. G. Makris, R. El-Ganainy, D. N. Christodoulides, M. Segev, and D. Kip, Observation of parity–time symmetry in optics, Nat. Phys. **6**, 192 (2010).

[7] A. Guo, G. J. Salamo, D. Duchesne, R. Morandotti, M. Volatier-Ravat, V. Aimez, G. A. Siviloglou, and D. N. Christodoulides, Observation of $\mathcal{PT}$-Symmetry Breaking in Complex Optical Potentials, Phys. Rev. Lett. **103**, 093902 (2009).

[8] S. Longhi, Parity-time symmetry meets photonics: A new twist in non-Hermitian optics, Europhys. Lett. **120**, 64001 (2018).

[9] C. M. Bender and S. Boettcher, Real Spectra in Non-Hermitian Hamiltonians Having $\mathcal{PT}$ Symmetry, Phys. Rev. Lett. **80**, 5243 (1998).

[10] P. A. Brandão and S. B. Cavalcanti, Non-Hermitian spectral changes in the scattering of partially coherent radiation by periodic structures, Opt. Lett. **44**, 4363 (2019).

[11] P. A. Brandão and S. B. Cavalcanti, Scattering of partially coherent radiation by non-Hermitian localized structures having parity-time symmetry, Phys. Rev. A **100**, 043822 (2019).

[12] M. A. Pinto and P. A. Brandão, Asymmetrical splitting in the spectrum of stochastic radiation scattered by non-Hermitian materials having $\mathcal{PT}$ symmetry, Phys. Rev. A **101**, 053817 (2020).

[13] R. A. Vieira and P. A. Brandão, Wolf effect in the scattering of polychromatic radiation by two spheres having parity-time symmetry, J. Opt. **22**, 125601 (2020).

[14] P. A. Brandão and O. Korotkova, Scattering theory for stationary materials with $\mathcal{PT}$ symmetry, Phys. Rev. A **103**, 013502 (2021).

[15] P. A. Brandão, J. P. Mendonça, and S. B. Cavalcanti, Low coherence-induced resonance in double-layer structures having parity-time symmetry, Opt. Lett. **46**, 717 (2021).

[16] O. Korotkova and P. A. Brandão, Light scattering from stationary $\mathcal{PT}$-symmetric collections of particles, Opt. Lett. **46**, 1417 (2021).

[17] D. G. Pires, N. M. Litchinitser, and P. A. Brandão, Scattering of partially coherent vortex beams by a $\mathcal{PT}$-symmetric dipole, Opt. Express **29**, 15576 (2021).

[18] X. Zhang, Y. Chen, F. Wang, and Y. Cai, Scattering of partially coherent vector beams by a deterministic medium having parity-time symmetry, Photonics **9**, 140 (2022).

[19] X. Zhang, Y. Liu, Y. Chen, F. Wang, and Y. Cai, Noncentrosymmetric far-zone spectral density induced by light scattering with random media having parity-time symmetry, Phys. Rev. A **105**, 023510 (2022).

[20] K. G. Makris, R. El-Ganainy, D. N. Christodoulides, and Z. H. Musslimani, Beam Dynamics in $\mathcal{PT}$ Symmetric Optical Lattices, Phys. Rev. Lett. **100**, 103904 (2008).

[21] V. V. Shkunov and D. Z. Anderson, Radiation Transfer Model of Self-Trapping Spatially Incoherent Radiation by Nonlinear Media, Phys. Rev. Lett. **81**, 2683 (1998).

[22] H. Buljan, G. Bartal, O. Cohen, T. Schwartz, O. Manela, T. Carmon, M. Segev, J. Fleischer, and D. Christodoulides, Partially coherent waves in nonlinear periodic lattices, special issue of Stud. Appl.ied Math. **115**, 173 (2005).

[23] F. Gori and M. Santarsiero, Devising genuine spatial correlation functions, Opt. Lett. **32**, 3531 (2007).

[24] A. Poddubny, I. Iorsh, P. Belov, and Y. Kivshar, Hyperbolic metamaterials, Nat. Photonics **7**, 948 (2013).

[25] A. E. Siegman, How to (maybe) measure laser beam quality, in *Diode Pumped Solid State Lasers: Applications and Issues* (Optica Publishing Group, Washington, DC, 1998), p. MQ1.

[26] M. Smith and G. Gbur, Coherence resonances and band gaps in plasmonic hole arrays, Phys. Rev. A **99**, 023812 (2019).

[27] G. L. Pedrola, *Beam Propagation Method for Design of Optical Waveguide Devices* (Wiley, New York, 2015).

[28] T. Hartmann, F. Keck, H. Korsch, and S. Mossmann, Dynamics of bloch oscillations, New J. Phys. **6**, 2 (2004).

[29] S. Longhi, Bloch Oscillations in Complex Crystals with $\mathcal{PT}$ Symmetry, Phys. Rev. Lett. **103**, 123601 (2009).

[30] J. M. Zeuner, M. C. Rechtsman, Y. Plotnik, Y. Lumer, S. Nolte, M. S. Rudner, M. Segev, and A. Szameit, Observation of a Topological Transition in the Bulk of a Non-Hermitian System, Phys. Rev. Lett. **115**, 040402 (2015).

[31] G. Della Valle and S. Longhi, Spectral and transport properties of time-periodic $\mathcal{PT}$-symmetric tight-binding lattices, Phys. Rev. A **87**, 022119 (2013).